SUPPLEMENTARY INFORMATION

Spectral Properties and Isomerisation Path of Retinal in C1C2 ChannelRhodopsin

Irina Dokukina and Oliver Weingart*

Geometry changes after optimisation

Figure S1 shows an overlay of the optimised ground state geometry (cyan) and ^1B_u –like structure (orange). The polyene chain twist observed in the ground state at the C13=C14 double bond persist after the optimisation in the excited ^1B_u –like state.

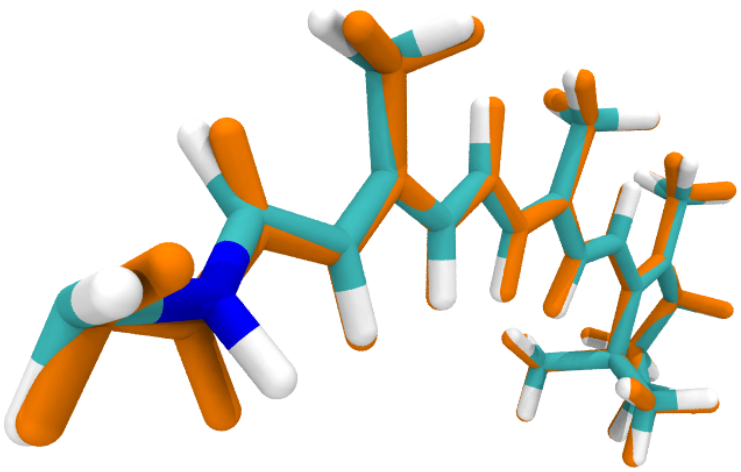

Figure S1: Overlay of S_0-CASSCF (cyan) and ^1B_u-CASSCF (orange) optimised geometries

Figure S2 shows bond lengths along polyene chain of retinal in the CASSCF optimised ground state geometries in standard (GLU) protonation with both counterions charged and alternative protonation (GLH) with protonated GLU162 residue. No significant changes can be noted for the bond pattern in alternative protonation.

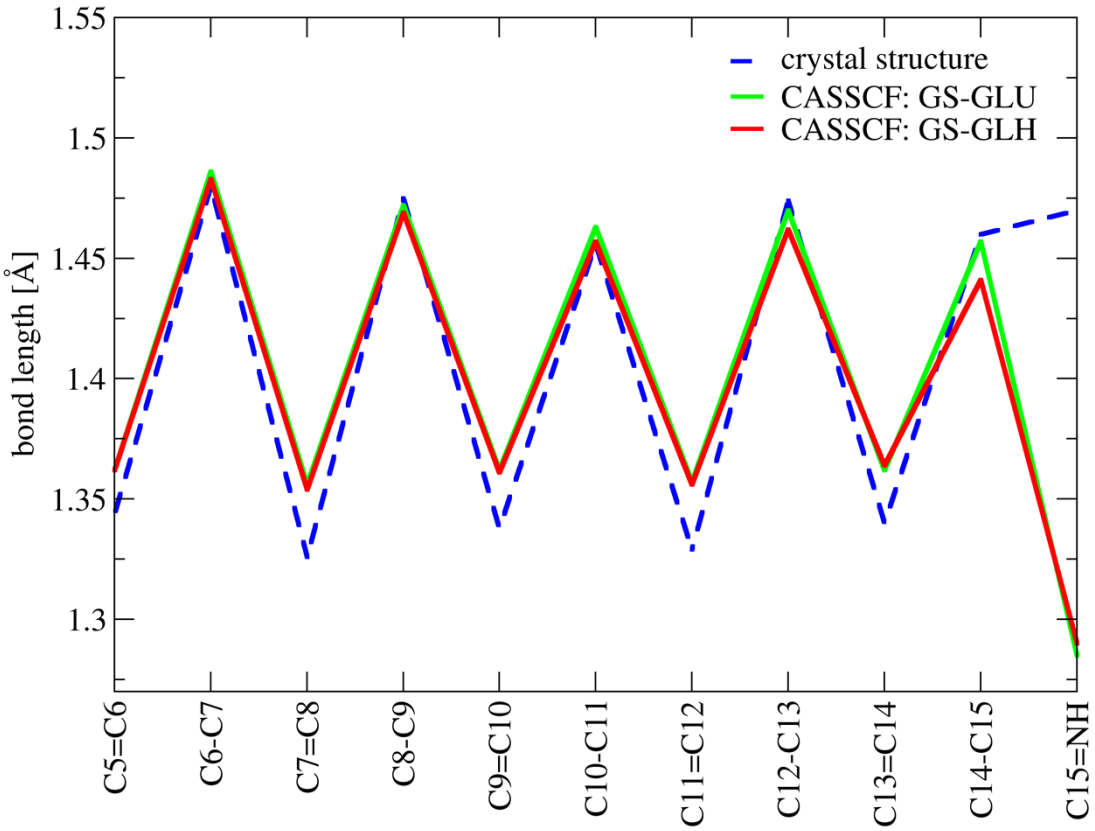

Figure S2: Bond lengths in crystal structure and CASSCF-optimised ground state geometries in standard (GLU) and alternative (GLH) protonation states of counterions.

Nature of low lying excited states for different protonation states

Standard Protonation

Tables S1-S3 show MS-CASPT2 and DFT/MRCI data for HF, DFT and CASSCF optimisations of retinal within frozen protein environment. For all geometries the MS-CASPT2 and DFT/MRCI S_0-S_1 excitation energy is blue shifted relative to structures with additionally optimised counter ions. Only the DFT/MRCI maximum absorption wavelength for the DFT geometry (see Table S2) is red shifted.

Table S1: Excitation energies and oscillator strengths for retinal optimised at the HF/Amber S_0 level with frozen protein environment. The experimental value for the maximum absorption is 2.64 eV.

Method	State	E(eV)	Config.	Weight	*f*
MS-CASPT2	S_0	0	GS	0.74	-
	S_1	2.6759	H→L	0.59	1.22
	S_2	4.2249	^{2}H→^{2}L	0.25	0.10
			H-1→L	0.16	
	S_3	5.2520	H-2→L	0.19	0.94×10^{-1}
			H-1/H→L	0.16	
	S_4	5.6173	H-3→L	0.20	0.39×10^{-3}
DFT/MRCI	S_0	0	GS	0.94	-
	S_1	2.9415	H→L	0.83	1.54
	S_2	3.7681	H-1→L	0.39	0.54
			H→L+1	0.11	
	S_3	4.3511	H→L+1	0.31	0.26
			H-1→L	0.18	
			H-2→L	0.10	
	S_4	4.6581	H-2→L	0.29	0.067
			H→L+1	0.22	

Table S2: Excitation energies and oscillator strengths for retinal optimised at the DFT-B3LYP/Amber S_0 level with frozen protein environment. The experimental value for the maximum absorption is 2.64 eV.

Method	State	E(eV)	Config.	Weight	*f*
MS-CASPT2	S_0	0	GS	0.72	-
	S_1	2.7866	H→L	0.37	1.12
			H-1→L	0.12	
	S_2	3.2989	H→L	0.23	0.55
			^{2}H→^{2}L	0.17	
			H-1→L	0.12	
	S_3	4.1606	H-2→L	0.18	0.11
			H-1/H→L	0.17	
	S_4	5.0274	H-3→L	0.20	0.59×10^{-2}
DFT/MRCI	S_0	0	GS	0.91	-
	S_1	2.5496	H→L	0.62	1.21
	S_2	2.8883	H→L	0.24	1.06
			H-1→L	0.19	
			^{2}H→^{2}L	0.15	
	S_3	3.6634	H-2→L	0.25	0.023
			H-1,H→L	0.16	
			H→L+2	0.11	
	S_4	4.1987	H-1→L	0.38	0.12
			H→L+1	0.36	

Table S3: Excitation energies and oscillator strengths for retinal optimised at the CASSCF/Amber S_0 level with frozen protein environment. The experimental value for the maximum absorption is 2.64 eV.

Method	State	E(eV)	Config.	Weight	F
MS-CASPT2	S_0	0	GS	0.72	-
	S_1	2.7467	H→L	0.54	1.16
	S_2	3.9286	^{2}H→^{2}L	0.23	0.14
			H-1→L	0.15	
	S_3	4.8719	H-2→L	0.17	0.17
			H-1/H→L	0.17	
	S_4	5.3833	H-3→L	0.19	0.33×10^{-2}
DFT/MRCI	S_0	0	GS	0.93	-
	S_1	2.8271	H→L	0.81	1.47
	S_2	3.5398	H-1 →L	0.34	0.60
			H→L+1	0.12	
	S_3	4.1534	H→L+1	0.25	0.23
			H-1→L	0.15	
			H-2→L	0.11	
	S_4	4.4816	H→L+1	0.25	0.075
			H-2→L	0.24	
			H-1→L	0.14	

Alternative Protonation

Additionally to standard protonation, a model with a protonated counter ion (E162) was created. After ground state optimisation the retinal geometry (Figure S3, orange) does not change with respect to the optimised geometry in standard protonation (Figure S3, cyan).

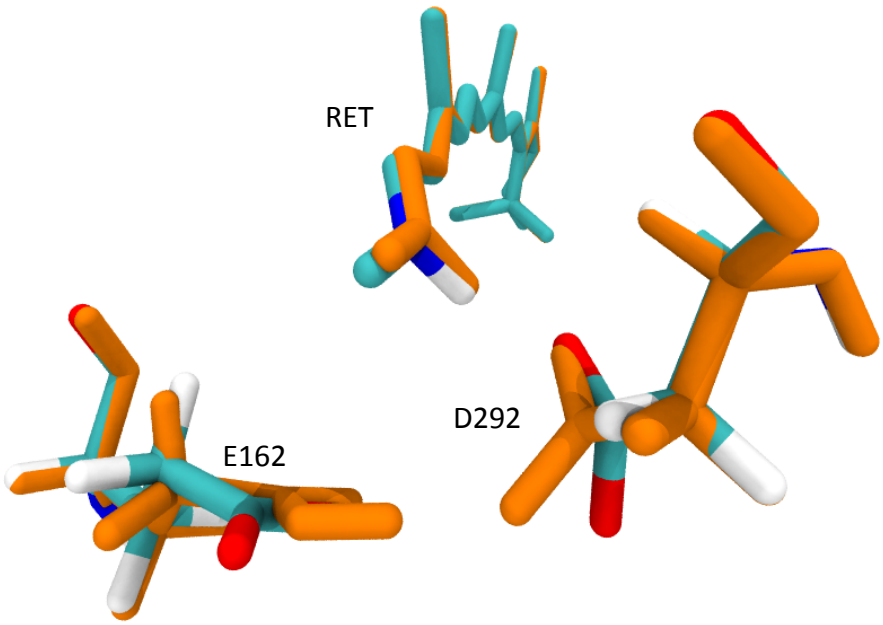

Figure S3: Overlay of S_0/CASSCF optimised retinal structure in standard protonation (cyan) and S_0/CASSCF optimised retinal structure in alternative protonation (orange).

The composition of the excited states (Tables S4-S5) changes only slightly with respect to the optimised geometry in standard protonation. The S_0-S_1 excitation energy is strongly red shifted for both DFT and CASSCF optimised geometries.

Table S4: Excitation energies and oscillator strengths for retinal in alternative protonation optimised at the DFT-B3LYP/Amber S_0 level with counter ions movable. The experimental value for the maximum absorption is 2.64 eV.

Method	State	E(eV)	Config.	Weight	*f*
MS-CASPT2	S_0	0	GS	0.75	-
	S_1	2.5517	H→L	0.39	1.65
			H-1→L+1	0.14	
	S_2	3.2347	^{2}H→^{2}L	0.21	0.62
			1H→L	0.21	
	S_3	4.0339	H-1→L	0.14	0.65×10^{-2}
			H-2→L	0.21	
			H-1/H→L	0.16	
			H→L/L+1	0.11	
			H→L+2	0.10	
	S_4	4.9848	H-3→L	0.24	0.44×10^{-2}
			H-2/H→L	0.11	
DFT/MRCI	S_0	0	GS	0.91	-
	S_1	2.2105	H→L	0.82	1.95
	S_2	2.6893	H-1→L	0.27	0.33
			^{2}H→^{2}L	0.24	
			H→L+1	0.11	
	S_3	3.5372	H-2→L	0.27	0.0035
			H-1,H→L	0.17	
	S_4	3.9227	H-1→L	0.39	0.078
			H→L+1	0.18	

Table S5: Excitation energies and oscillator strengths for retinal in alternative protonation optimised at the CASSCF/Amber S_0 level with counter ions movable. The experimental value for the maximum absorption is 2.64 eV.

Method	State	E(eV)	Config.	Weight	*f*
MS-CASPT2	S_0	0	GS	0.75	-
	S_1	2.4197	1H→L	0.53	1.54
			H-1→L+1	0.11	
	S_2	4.0700	^{2}H→^{2}L	0.28	0.22
			H-1→L	0.16	
	S_3	4.6387	H-2→L	0.18	0.17×10^{-2}
			H-1/H→L	0.14	
			H→L/L+1	0.11	
			H→L+2	0.10	
	S_4	5.3165	H-3→L	0.22	0.2×10^{-2}
DFT/MRCI	S_0	0	GS	0.94	-
	S_1	2.3668	H→L	0.84	1.54
	S_2	3.3872	H-1→L	0.52	0.46
	S_3	3.9782	H→L+1	0.31	0.25
			H-1→L	0.14	
			H-2→L	0.13	
	S_4	4.3835	H-2→L	0.25	0.055
			H→L+1	0.11	

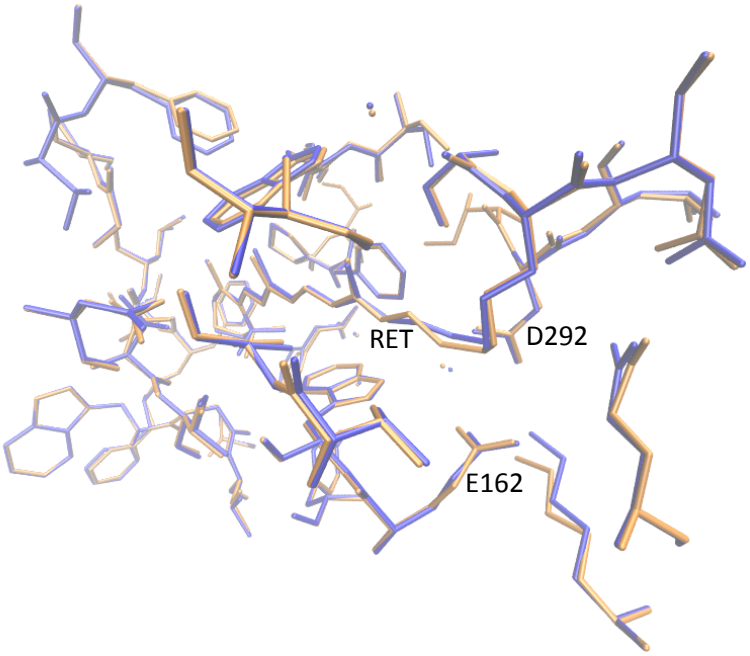

Figure S4: Crystal structure (orange) and structure after optimisation with movable pocket residues (blue)

Optimisation with movable binding pocket

The CASSCF optimized C1C2 geometry was re-optimized, but now with all residues movable within a distance of 5 Angstrom of the retinal chromophore. Figure S4 shows an overlay of the optimised structure with the crystal structure. We note only minor changes for the positions of the pocket residues. The orientation of the NH^+ group of retinal still points towards D292 after optimisation. Excitation energies computed at the MS-CASPT2 level of theory are reported in Table S6.

Table S6: MS-CASPT2 excitation energies and oscillator strengths for retinal optimised at the CASSCF/Amber S_0 level with pocket residues movable.

State	E(eV)	Config.	Weight	*f*
S_0	0	GS	0.73	-
S_1	2.5696	H→L	0.55	1.18
S_2	3.9468	^{2}H→^{2}L	0.24	0.11
		H-1→L	0.16	
		H→L+1	0.09	
		H→L	0.08	
S_3	4.9890	H-2→L	0.18	0.12
		H-1/H→L	0.16	
		H→L/L+1	0.08	
		H→L+2	0.08	
S_4	5.4072	H-3→L	0.19	0.75×10^{-3}

	H→ L+3	0.09

Salt bridge to E162

A structure with the retinal NH^+ proton forming a salt bridge with the E162 counter ion was obtained by the following strategy: the missing LOOPS in the crystal structure were modelled with the program Modeller. The resulting structure was then optimised with all residues within a 5 Angstrom distance of retinal movable, using HF/6-31G* as QM method. Figure S5 shows an overlay of this structure and the corresponding CASSCF-optimised structure with mobile binding pocket (without LOOP refinement, see Fig. S4). Larger re-arrangements of the mobile residues with respect to the crystal structure are apparent in this structure. MS-CASPT2 computed absorption data is shown in Table S7. A similar absorption wavelength is obtained as for the D292 bound geometry.

Figure S5: Overlay of CASSCF optimized structure forming a salt bridge to D292 (blue) and HF-optimized structure with salt bridge to E162 (orange). NH-O distances in Å.

Table S7: MS-CASPT2 excitation energies and oscillator strengths for C1C2 optimised at the HF/Amber S_0 level with pocket residues movable, with retinal forming a salt bridge to E162.

State	E(eV)	Config.	Weight	*f*
S_0	0	GS	0.75	-
S_1	2.6212	H→L	0.60	1.27
S_2	4.2362	^{2}H→^{2}L	0.26	0.10
		H-1→L	0.16	
		H→L+1	0.09	
S_3	5.2799	H-2→L	0.18	0.02
		H-1/H→L	0.14	
		H→L/L+1	0.10	
		H→L+2	0.09	
S_4	5.6301	H-3→L	0.20	0.14×10^{-2}

H→ L+3	0.09	

Properties after ^1B_u excitation

Table S8 shows MS-CASPT2 data for ^1B_u CASSCF optimisation of retinal with counter ions and water molecule movable. The bright (f=1.69) S_1 state is defined by ca. 50% HOMO-LUMO excitation with an emission wavelength of 489 nm. The dark S_2 state is mostly defined by HOMO-LUMO double excitation and lies close to S_1 state. Other excited states are well separated and only S_3 has significant oscillator strength.

Table S8: MS-CASPT2 excitation energies and oscillator strengths for retinal optimised at the CASSCF/Amber S_1 level with counter ions and water molecule movable.

State	E(eV)	Config.	Weight	f
S_0	0	GS	0.73	-
S_1	2.5347	H→L	0.50	1.69
S_2	2.8498	^{2}H→^{2}L	0.24	0.91×10^{-1}
		H-1→L	0.16	
		H→L+1	0.11	
		H→L	0.08	
S_3	4.0638	H-2→L	0.16	0.12
		H→L/l+1	0.12	
		H-1/H→L	0.11	
		H→L+2	0.11	
S_4	4.8236	H-3→L	0.13	0.72×10^{-2}
		H-2→H/L	0.11	

Properties of 13-cis retinal in C1C2

MS-CASPT2 and DFT/MRCI calculations were performed (Table S9) to compare 13-*cis* and all-*trans* retinal ground state structures. Their state compositions are very similar. S_0-S_1 excitation energy is red shifted by 12 nm at the MS-CASPT2 level and 17 nm at DFT/MRCI level. After optimisation, the salt bridge to D292 is released, and the retinal Schiff base NH^+ proton points towards the neighboring serine 295 residue (see Figure S6).

Table S9: Excitation energies and oscillator strengths for 13-*cis* retinal optimised at the CASSCF/Amber S_0 level with counter ions movable.

Method	State	E(eV)	Config.	Weight	*f*
MS-CASPT2	S_0	0	GS	0.74	-
	S_1	2.5348	H→L	0.53	1.38
			H→L+1	0.11	
	S_2	3.9097	^{2}H→^{2}L	0.26	0.13
			H-1→L	0.16	
	S_3	4.9140	H-2→L	0.18	0.17×10^{-4}
			H/H-1→L	0.14	
			H→L/L+1	0.11	
			H→L+2	0.11	
	S_4	5.3784	H-3→L	0.21	0.36×10^{-2}
DFT/MRCI	S_0	0	GS	0.93	0
	S_1	2.6414	H→L	0.81	1.48
	S_2	3.4106	H-1→L	0.37	0.47
			^{2}H→^{2}L	0.11	
			H→L+1	0.10	
	S_3	3.9743	H→L+1	0.29	0.27
			H-1→L	0.17	
	S_4	4.3553	H-2→L	0.28	0.05
			H→L+1	0.19	
			H-1→L	0.11	

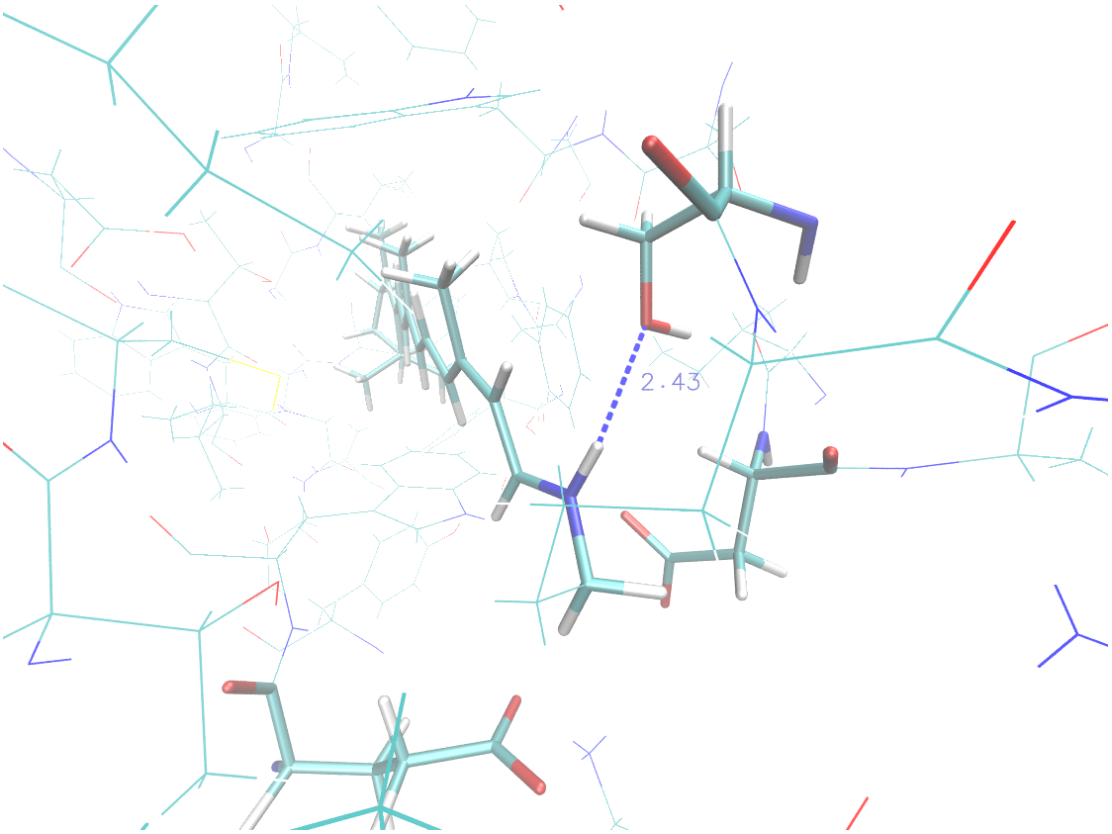

Figure S6: Structure of CASSCF optimised 13-*cis* retinal in C1C2 binding pocket, with the Schiff base NH^+ moiety oriented towards S295. The NH-O distance is given in Å.

Effect of bond length alternation on retinal absorption in vacuo and in C1C2

The charged protein environment in C1C2 leads to a different effect of bond length alternation on the excited state absorption. This is also documented in Figure 5 of the main text, where the MS-CASPT2 computed absorption of a DFT optimised structure with less bond alternation shifts to higher energies compared to the corresponding CASSCF structure. Usually, reduced bond length alternation will lead to a red shift in absorption. The underlying process is discussed in the following.

Different from uncharged polyenes, HOMO-LUMO excitation in protonated Schiff bases relocates part of the positive charge situated at the N-terminus towards the β-ionone ring. This becomes apparent in Figure S7, where a charge of ca. +0.4 electrons migrates from the right to the left half of the chromophore after excitation. In vacuum, the β-ionone part carries a positive charge after excitation to the absorbing S_1 state. The charge transport is of similar magnitude in DFT and CASSCF computed structures. The influence of bond length alternation on the MS-CASPT2 vacuum state energies is shown in Figure S8. In the DFT optimized structure both states decrease in energy, but the excited state somewhat more than the ground state, as the electronic structure of a strongly conjugated system is

more similar to the relaxed S_1 geometry with inverted bond length alternation. This leads to the known red-shift in absorption wavelength when conjugation is enhanced.

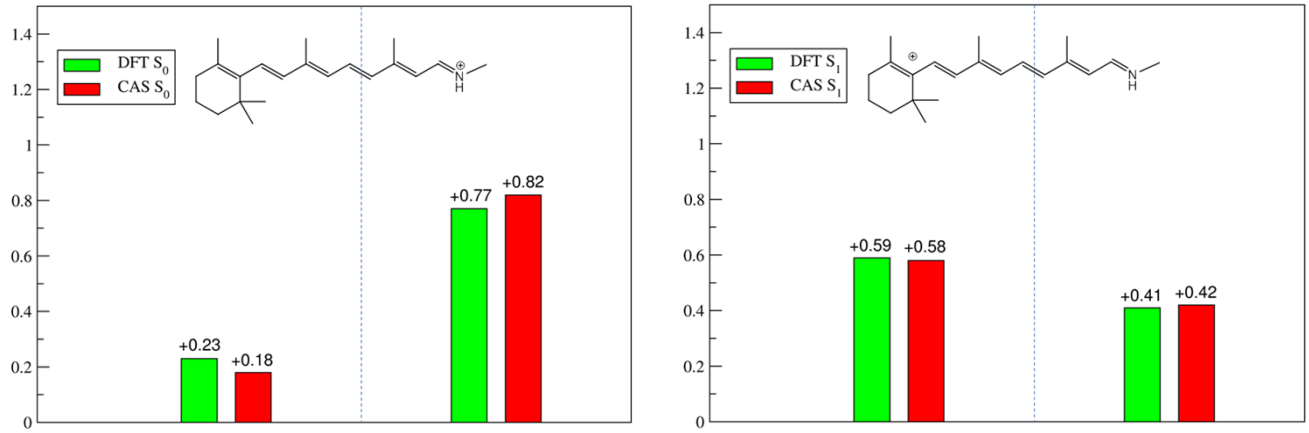

Figure S7: Charges of chromophore halfs in ground and HOMO-LUMO excited state for DFT and CASSCF optimized C1C2 retinal structures in vacuo.

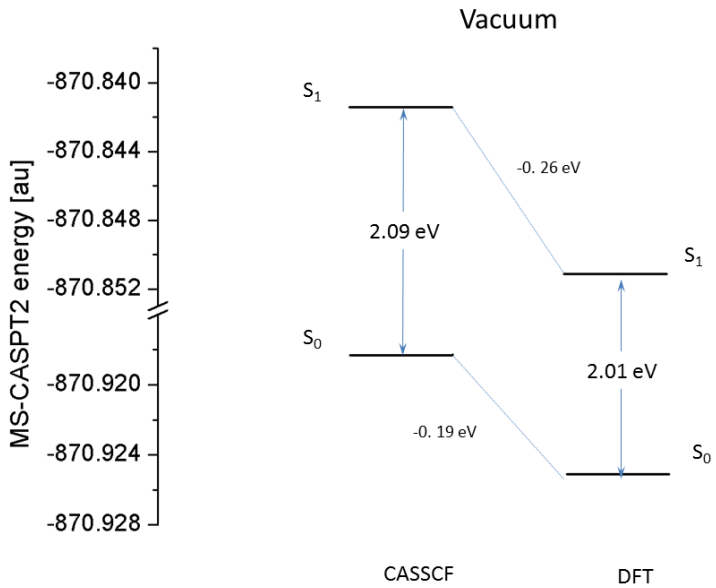

Figure S8: MS-CASPT2 energies of retinal ground state and first excited state in CASSCF and DFT-optimised C1C2 strutures without surrounding.

In the protein environment, relocation of the positive charge is hindered by the negatively charged counterions near the N-terminus of retinal (Figure S9). In the ground state, the positive charge is almost entirely located near the N-terminus. An alternating structure is preferred within the charged environment, the conjugated DFT structure is slightly destabilised (Figure S10). Upon HOMO-LUMO excitation, only a small amount of charge shifts towards the β-ionone ring compared to vacuum. In the conjugated DFT structure, we note that slightly more charge (ca +0.1 electron) is transported against the electrostatic field as in the alternating CASSCF structure. Together with energy splitting due to state mixing (see next chapter) this effect may contribute to the destabilisation of the excited state energy in the DFT structure (Figure S10) and to the observed blue shift in absorption wavelength.

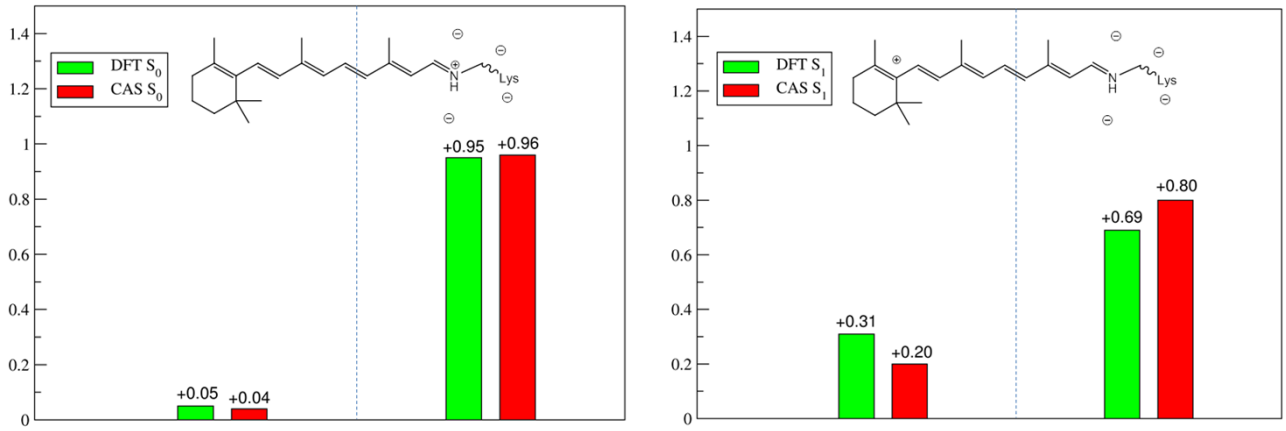

Figure S9: Charges of chromophore halfs in ground and HOMO-LUMO excited state for DFT and CASSCF optimized structures in protein environment.

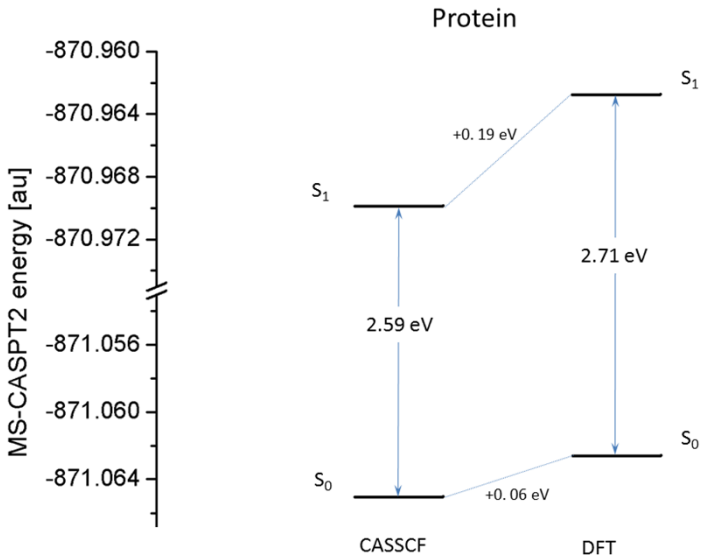

Figure S10: MS-CASPT2 energies of retinal ground state and first excited state in CASSCF and DFT-optimised C1C2 strutures in the protein environment.

SS-CASPT2 vs. MS-CASPT2

Figure S11 compares the excitation energies in C1C2 retinal obtained by single and multistate CASPT2 computations. The single state energies strongly deviate from the MS-CASPT2 description. In single state, the HOMO-LUMO excitation to the state is strongly blue-shifted, and it appears in the S_2 state. The lowest state in this description is the ^2A_g-like state associated with HOMO-LUMO double excitation, S_3 and S_4 states are stabilised. If the states are allowed to interact in the multistate protocol, S_1 becomes the bright HOMO-LUMO excited state with good agreement to the experimental value. S_2 is upshifted, and also the oscillator strengths of this and higher states differ from the single state values. Table S10 shows the MS-CASPT2 coupling matrix, describing the contribution of the corresponding single state wavefunctions in the multistate treatment. As apparent from the off-diagonal elements, strong mixing occurs in comparison to the same values computed for the retinal chromophore without protein surrounding (Table S11), especially for the S_1, S_2 and S_3 states. The situation does not significantly change, when the nearby protein residues are allowed to relax. The diagonal elements in the vacuum computation indicate much more similarities in single and multistate treatment and thus only minor contribution due to state mixing.

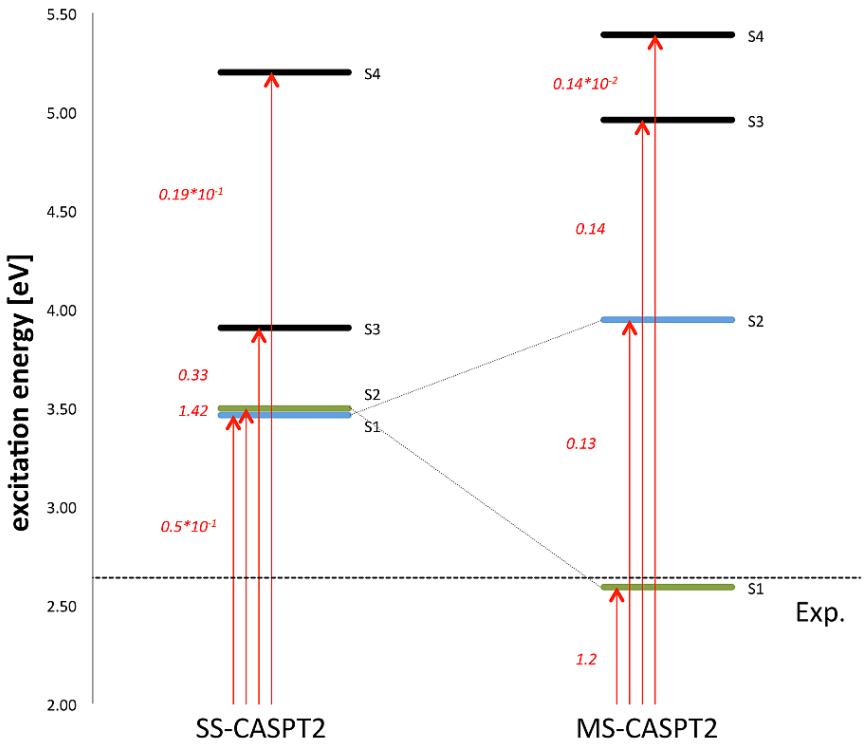

Figure S11: Excitation energies and oscillator strengths of retinal in C1C2 at single state and multistate CASPT2 level.

Table S10: SS-CASPT2 coupling coefficients for CASSCF-optimised retinal structure computed in protein environment

State	1	2	3	4	5
1	0.96875851	0.24296495	0.03527090	0.03434745	0.00715471
2	0.08306823	-0.46878480	0.87637558	0.07282017	0.00188344
3	-0.12107917	0.53785097	0.36161432	-0.75002472	-0.05248017
4	0.19915028	-0.65321348	-0.31464418	-0.64169374	-0.15125973
5	0.01690000	-0.07236937	-0.03091807	-0.13859851	0.98707223

Table S11: SS-CASPT2 coupling coefficients for CASSCF-optimized retinal structure computed in vacuum

State	1	2	3	4	5
1	0.97906369	-0.18127462	-0.08849572	-0.02360742	-0.01360126
2	-0.18485031	-0.96193594	-0.09829880	0.14541878	-0.09849024
3	0.07885328	-0.02755976	0.89388707	0.31081453	-0.31206225
4	-0.02841510	-0.14291553	0.25731834	-0.93620336	-0.18994280
5	0.01547226	-0.14364667	0.34243105	-0.07220566	0.92555581

CASSCF potential energy surfaces at CASSCF level

The CASSCF energy profiles for the S_0-S_4 states along the computed torsion path in the S_3 state is shown in Figure S12. Also indicated is the percentage of the leading configuration for S_3 (HOMO-LUMO single excitation) and S_1 (HOMO-LUMO double excitation). The S_2 state is highly mixed at the CASSCF level. The S_3 state was used for geometry optimisation.

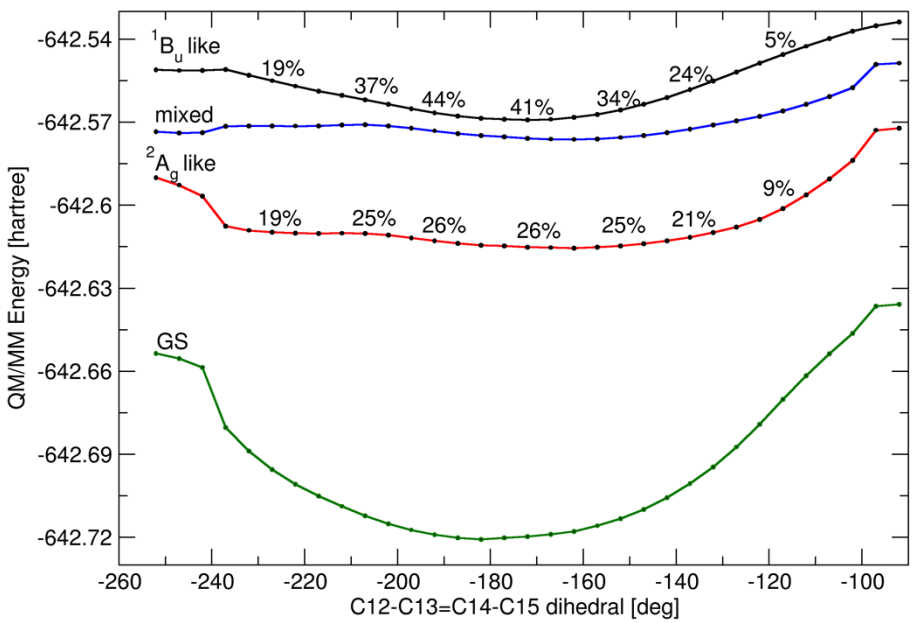

Figure S12: Computed CASSCF energy profiles for torsion in S_3 along the C13=C14 bond.

Charge translocation along ^1B_u-like isomerisation paths

Figure S13 provides CASPT2 computed charges along the isomerisation paths of the chromophore fragments right and left of the isomerising C13=C14 double bond. Notice that this is a different fragmentation as the one shown in figure S9, where for illustration the cut was placed among the C11=C12 bond. The S_0 and S_1 values for the FC geometry are also given in table S12. The Figure shows that the positive charge, which resides in the β-ionone fragment after excitation, is effectively transported back towards the Schiff base tail along both isomerisation coordinates. In the negative path, the β-ionone fragment becomes initially more positive, in-line with the occurrence of a barrier in this direction.

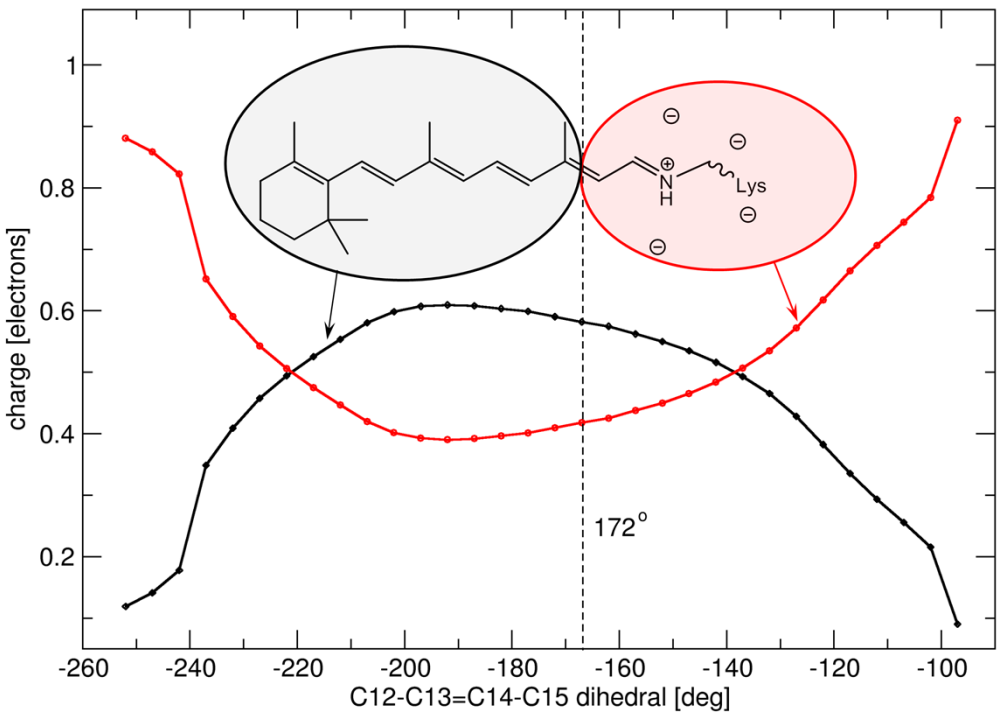

Figure S13: Charge of chromophore fragments along computed isomerisation pathways. The vertical line denotes the start of the computed path at -172° twist.

Table S12: Charges of chromphore fragments in S_0 and S_1 states at the FC point and bond-relaxed ^1B_u-like structure (starting point in Figure S13).

Structure	FC		^1B_u-like	
State	S_0	S_1	S_0	S_1
β-ionone fragment [e]	+0.227	+0.499	+0.274	+0.590
Schiff-base fragment [e]	+0.773	+0.501	+0.726	+0.410

Resonance Raman spectra of all-*trans* and 13-*cis* retinal in C1C2

Assigned resonance Raman modes and frequencies are listed in the Table S12-S13.

Table S13 Frequencies and mode assignments for optimised all-*trans*-retinal in C1C2 (Intensity > 0.05)

Freq. [cm^{-1}]	Scaled (* 0.877)	Intensity	Mode
852	747	0.14	H2O wagging
908	797	0.07	H11-12 OOP asym.
920	807	0.06	NH asym. OOP
938	823	0.14	H12-H14 ip. bending, C1-Me wagging
978	858	0.97	H14 OOP, H11 asym. OOP
993	870	0.13	Lys-C18/C19-CH2 rocking
1012	887	0.07	Lys-C18-C19 stretching, C18/C19-CH2 wagging, H17 ip bending
1059	929	0.09	N-H ip bending, H15 OOP, C17-CH2 wagging
1066	935	0.34	H11-H12 OOP sym.
1105	969	0.53	C5-C9-C13-Me rocking, C1-Me rocking, H7 OOP
1106	970	0.32	H15/N-H sym. OOP
1112	975	0.31	H7 OOP, C1-Me rocking
1129	990	2.75	C13-Me rocking;
1151	1009	0.08	C9-Me rocking
1167	1023	0.40	C13-Me rocking, C16-methylene wagging,
1176	1031	0.16	C13-Me rocking, C16-methylene wagging
1200	1052	0.46	C5-Me und C-9 Me wagging, C6-C7 stretching, C1-Me rocking
1219	1069	0.17	Lys-Me rocking
1222	1072	0.41	H8/H7 OOP, C2-CH2 twisting, C1-Me wagging
1242	1089	1.38	C9-Me rocking, C10-C11 stretching, H10-H11 asym. bending, H11-H12 asym. bending, C13-Me rocking, H14-H15 bending, C1-Me

			rocking
1268	1112	3.65	C4-methylene twisting, Lys-C17-methylene twisting, Lys-C19-methylene twisting,
1258	1103	0.48	Lys-C17/C19-CH2 twisting
1263	1108	0.59	C2-CH2 twisting
1266	1110	1.06	C14-C15 stretching, Lys-Lys-C17-CH2 twisting, C4-CH2 twisting
1268	1112	1.59	C4-CH2 twisting, Lys-C17/C19-CH2 twisting
1272	1115	1.04	Lys-C19-CH2 twisting
1284	1126	0.10	H8/H7 symm. OOP, C4-CH2 twisting, C1-C(Me) stretching, C2-CH2 wagging, C1-Me wagging
1325	1162	0.51	C5-Me stretching, C4-methylene wagging,
1342	1177	0.69	Lys-H20 bending
1343	1178	2.51	H10,H11,H12 bending
1361	1193	6.04	H14 bending
1392	1221	0.14	Lys-C18-CH wagging, Lys-C19-CH2 wagging, Lys-C20-CH wagging
1414	1240	1.16	H11 bending
1419	1244	0.27	C4-CH2 scissoring, C3-CH2 wagging, C2-CH2 wagging
1451	1272	0.09	C12 C13 C17- +C18-methylene wagging +bending
1466	1286	0.26	H7,H8, H10 ip. bending; C1-Me scissoring
1481	1299	0.19	H7 ip. bending
1487	1304	0.06	Lys-C17-CH2 scissoring
1490	1307	0.23	C1 asymm. methylene scissoring, C4-methylene scissoring
1496	1312	0.08	C1-Me scissoring
1497	1313	0.11	C4-CH2 scissoring, C1-Me scissoring
1504	1319	0.74	H10-H12 bending, H12-

			H14 asym. Bending, (H14-H15-NH bending)
1517	1330	0.07	C4-CH2 wagging + scissoring, C3/C2-CH2 scissoring,
1543	1353	0.10	H8-H10 asymm. Bending, C9-Me HOOP, C2-Me scissoring, H19-NH bending,H15 bending
1559	1367	0.09	C2/C3-CH2 scissoring, C1-Me (left) scissoring,
1561	1369	0.29	C9-Me scissoring, Lys CH2 bending, H15 ip bending
1574	1380	0.20	Lys-C18-methylen scissoring, H14-H15-bending, Lys-C16-methylene scissoring
1597	1401	0.12	C13-Me scissoring
1622	1422	0.11	C16-methylene twisting, C18- + C19-methylene wagging
1631	1431	0.10	C13-Me scissoring
1640	1438	0.13	C13-Me scissoring, Lys-C16-CH2 scissoring
1641	1440	0.28	C13-Me asym. scissoring, Lys-C16-methylen scissoring
1645	1443	0.12	C9-Me scissoring
1653	1450	0.11	C1-Me (left) scissoring
1655	1452	0.15	C9-Me asym. scissoring
1667	1462	0.09	C5-Me scissoring
1671	1466	0.10	N-H bending, Lys-C16-CH2 twisting
1673	1467	0.75	C1-Me scissoring, Lys-C16-methylene twisting, H7-H8 bending, H8-H10 asymm. bending, C7=C8 stretching
1737	1523	0.36	C4-C5 C6-C1 stretching C4-methylen wagging
1765	1548	4.93	C9=C10/C11=C12 stretching, H10/H11/H12 ip.

			bending, C13=C14 stretching (weak)
1769	1551	13.79	C13=C14 stretching
1797	1576	0.22	H7/H8 asymm. ip. bending, C7=C8/C9=C10 stretching
1848	1621	0.18	C5=C6 stretching, H7/H8 asymm. ip. bending
1891	1658	1.95	C15=N stretching, Lys-C16-CH2 scissoring
1959	1718	0.97	C15=N stretching, Lys-C16-CH2 scissoring

Table S14: Frequencies and mode assignments for optimised 13-cis retinal in C1C2 (intensity > 0.05).

Freq. [cm^{-1}]	Scaled (*0.877)	Intensity	Mode
839	735	0.07	HN OOP, Lys-C17-C18-C19-CH2 rocking
873	766	0.06	C2-CH2 rocking, C4-CH2 rocking,C9-C(Me) stretching
892	782	0.22	C2/C4-Me rocking, H12 OOP (weak)
940	824	1.34	H12 ip. bending, C1-Me scissoring
954	836	1.10	H2O wagging, H12 ip. bending
959	841	0.12	H2O wagging
973	853	0.21	H10 OOP
985	864	0.11	H14-OOP
998	875	0.09	Lys-C17-CH2 twisting, Lys-C18-C19 stretching, Lys-C18/C19-CH2 wagging
1018	893	0.13	Lys-C18-CH2 twisting
1063	933	0.11	H11/H12/H15 sym. OOP
1076	944	0.09	H15-OOP; C19 (lys.) scissoring
1112	975	0.18	C5/C9-Me rock; H7 OOP
1137	997	1.28	H15/N-H- OOP; Lys-C16-CH2 twisting, Lys-C17-CH2 twisting
1150	1008	0.51	C9-Me scissoring
1155	1013	0.40	C9-Me rocking
1176	1032	1.21	C13-Me rock, C14-C15 stretching, H15 ip bending
1210	1061	0.20	C13-Me rock, C3-CH2 twisting, C1-Me scissoring
1226	1075	0.69	C13-Me rock, C2-CH2 twisting, C1-Me scissoring
1235	1083	0.80	C13-Me rock, C3-CH2 twisting
1253	1099	1.49	H15 ip bending, Lys-C16/C17-CH2 bending
1286	1128	1.18	H7/H8 OOP

1295	1136	2.08	C10-C11 stretching, C4-CH2 twisting, Lys-C18-CH2 twisting
1325	1162	3.35	H10/H12 ip. bending, C4-CH2 scissoring
1332	1168	1.16	C4-CH2 wagging, H10/H12 ip bending, H20 ip. bending
1333	1169	0.15	H20 ip. bending
1383	1213	0.55	C13-C(Me) stretching, H12/H14 bending, C13-Me-H bending
1441	1264	0.12	H15 ip bending, Lys-C17-CH2 scissoring
1459	1280	0.14	H15 ip bending, Lys-C18/C19-CH2 scissoring, H20 ip bending
1481	1299	0.78	C1-Me rocking (right), H7 ip. bending, Lys-C17-CH2 scissoring
1489	1305	1.07	H7/H11 ip bending
1497	1313	0.61	H11 ip. bending, C4/C2-CH2 scissoring, C1-Me scissoring
1510	1325	0.41	H10-H11 ip. bending, C1-Me scissoring
1569	1376	0.74	NH ip. bending, Lys-C18 scissoring
1577	1383	1.63	H14/NH ip. bending, Lys-C16/C18-CH2 scissoring
1631	1430	0.77	H14 ip. bending, C16-CH2 scissoring, C13-Me scissoring
1650	1447	0.37	C13-Me scissoring; C16-CH2 scissoring, NH ip bending
1655	1452	0.13	C9-Me scissoring, C13-Me scissoring (weak)
1670	1464	0.11	C1-Me scissoring (left)
1683	1476	0.79	C1-Me scissoring (right)
1718	1506	1.09	H14/N-H ip. bending; C13-Me scissoring

1738	1524	0.25	β-ion.: C4-C5 + C1-C6 stretching, C4-methylene wagging
1778	1560	7.94	C11-C12 stretching, C9-C10 stretching; H10-H11-H12 ip. bending
1799	1578	5.73	C13=C14 stretching, H14 ip. bending, H7-H8 asym. ip. bending
1805	1583	2.71	H8 ip bending, C13-C14 stretching, H14 ip bending
1871	1641	2.79	C15-N stretching, H15-NH asym. bending, Lys-C16-CH2 scissoring
1901	1667	0.94	C16-CH2 scissoring; C15-N stretching, H-N ip bending

Table S15 shows modes assigned by Nack et al. for the experimental ChR2 spectrum.

Table S15: ChR2 modes assigned by Nack et al. (ref. 12 in the paper).

Freq. [cm^{-1}]	Mode
823	HOOP
845	HOOP
1001	in-plane rocking of two methyl groups at C9 and C13
1061	all-*trans* C-C stretchinging
1088	C-C stretchinging of gauche modes
1125	all-*trans* C-C stretchinging
1183	contributions of 13-*cis* retinal
1200	all-*trans* characteristic band
1270	CCH in plane rocking of vinyl hydrogens
1440	methylene scissoring
1551	symmetric C=C stretchinging mode of retinal
1657	C=N stretching of the Schiff base

IR difference spectra of all-trans and 13-cis C1C2

Figure S14 shows the computed IR difference spectra of the optimised 13-*cis* and all-*trans* retinal structures in C1C2 in comparison with the experimental data by Furutani et al. [ref 40 in the paper] The computed line spectra were convoluted with a Lorentz shaped function (5 cm^{-1} FWHM) before taking the difference. Prominent bands representing changes in Schiff base C=N and C=C stretching modes match well with the experimental findings. For band assignments see also resonance Raman data.

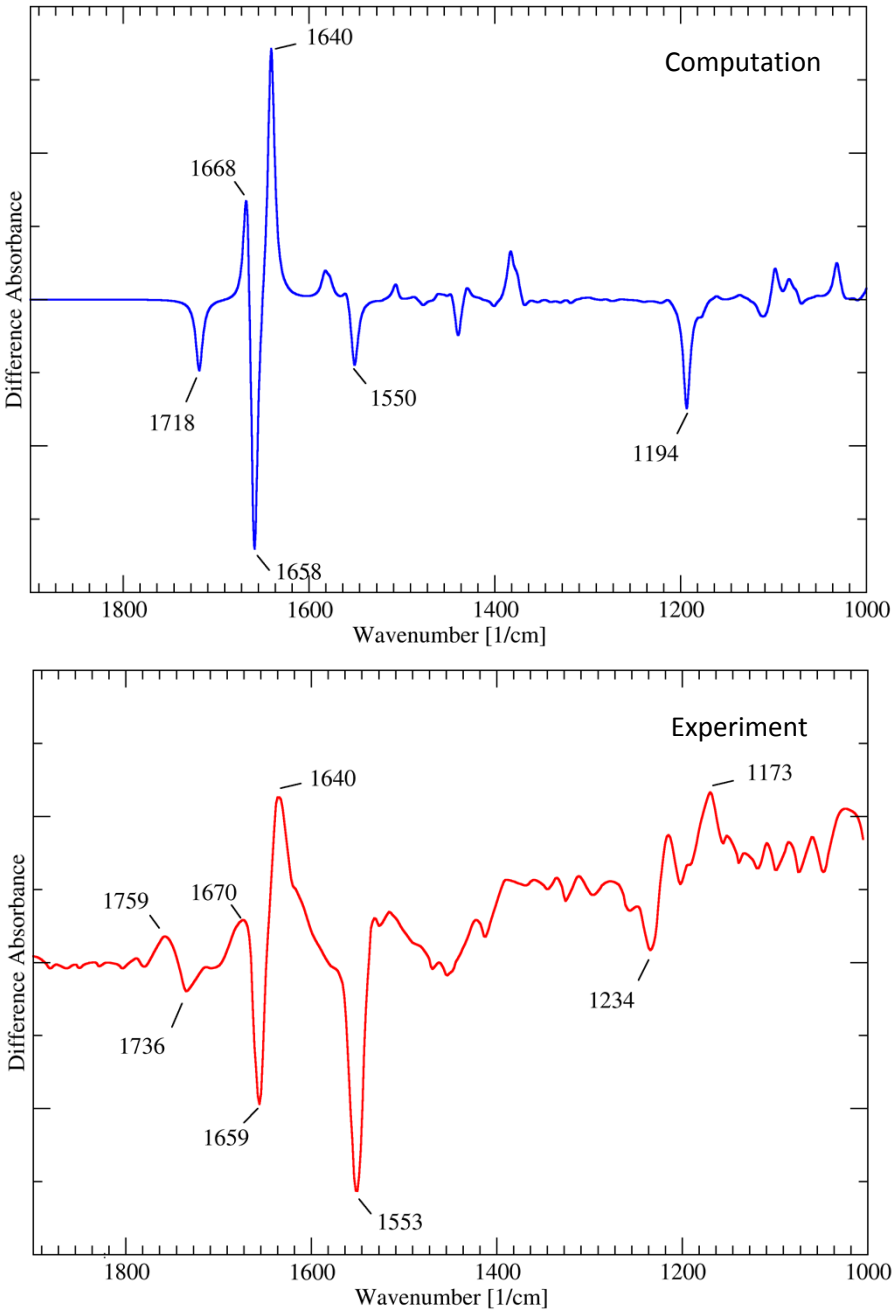

Figure S14: computed IR difference spectrum (above) and experimental result from Furutani and coworkers, reproduced from data in Fig. 8a of reference [40] in the paper.

Forces after HOMO-LUMO excitation

Figure S15 and Figure S16 show force vectors in all-*trans* and 13-*cis* retinal after vertical excitation to the ^1B_u–like state.

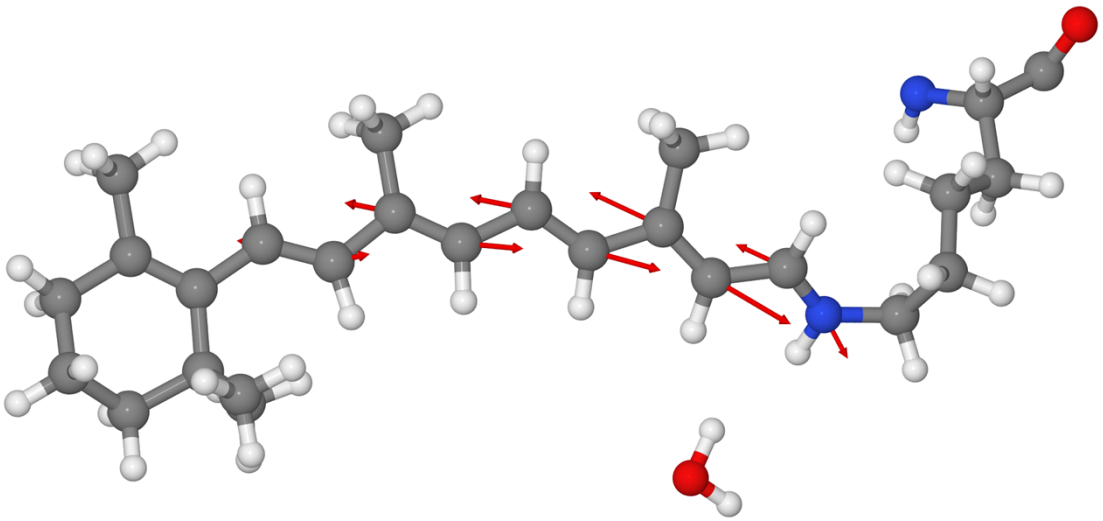

Figure S15: Atomic forces after vertical excitation in the all-*trans* retinal optimised geometry.

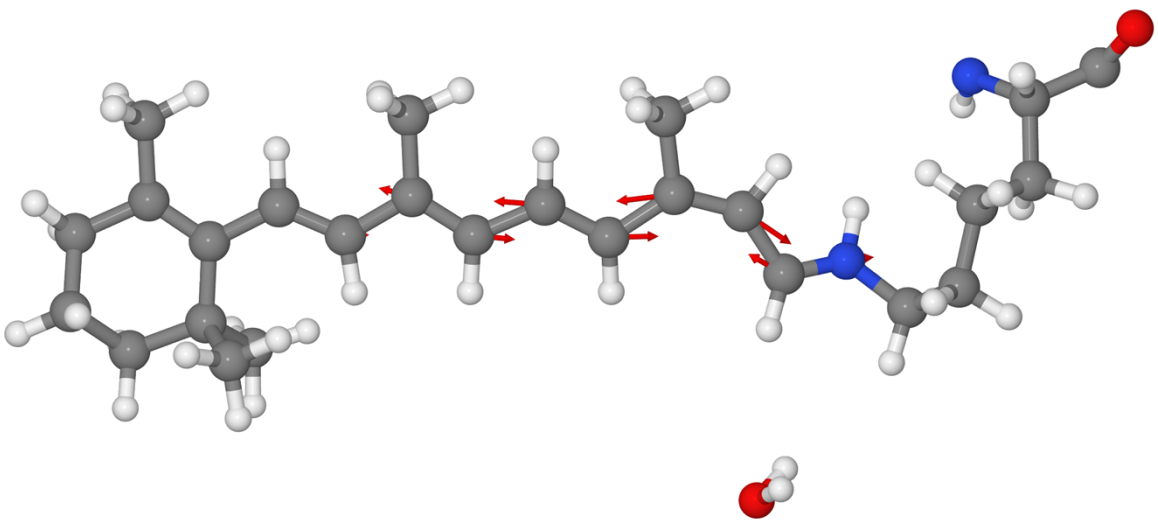

Figure S16: Forces after vertical ^1B_u–like excitation in the 13-*cis* retinal optimised geometry.

Influence of the electrostatic environment on retinal absorption

To investigate the influence of the electrostatic environment on retinal absorption, twelve protein residues in the vicinity of the retinal chromophore were selected (Figure S17).

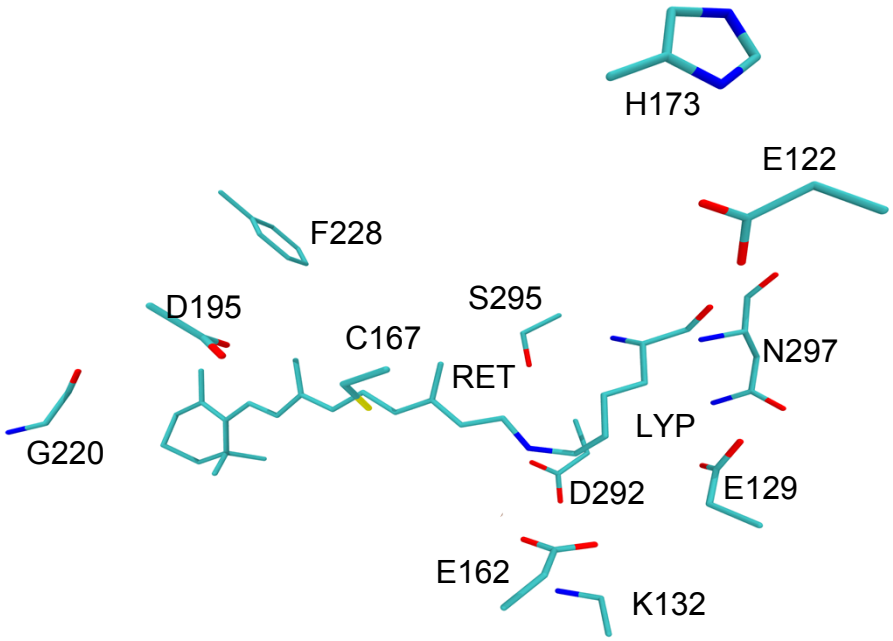

Figure S17: Location of amino acids regulating retinal absorption.

Coordinates of optimised geometries

Table S16: Coordinates of the all-*trans* S_0-CASSCF optimised geometry

Residue Name	Atom Name	x	y	z
E162	N	7.466808	32.349233	19.920353
	H	7.62654	31.408851	19.575532
	C	8.362653	33.416995	19.41741
	H	8.872387	33.87274	20.268553
	C	9.439089	32.891995	18.437634
	H	10.130509	32.242384	18.978521
	H	8.951324	32.27688	17.683998
	C	10.237212	34.02715	17.734696
	H	9.575569	34.759678	17.267194
	H	10.839796	34.562812	18.473617
	C	11.09998	33.488621	16.618971
	O	10.575063	32.700912	15.799877
	O	12.292736	33.852806	16.556715
	C	7.580934	34.510728	18.726468
	O	7.848195	35.683059	18.903266
D292	N	12.042608	34.837237	9.046666
	H	12.152875	33.844232	8.879225
	C	12.503682	35.333422	10.366398
	H	11.700542	35.926977	10.804745
	C	12.833045	34.192913	11.374376
	H	13.539447	33.501744	10.913209
	H	13.344053	34.619582	12.239616
	C	11.61555	33.407137	11.894049
	O	11.756639	32.232354	12.31082
	O	10.515263	34.012584	11.996968
	C	13.695178	36.267867	10.207756
	O	13.769484	37.332394	10.790316
LYP	N	12.695722	39.898305	11.282804
	C	13.285196	40.322242	12.57453
	C	14.600764	41.028471	12.375266
	O	14.757054	42.178544	12.735863
	C	13.370285	39.162551	13.591247
	C	11.981871	38.911138	14.215166
	C	11.883204	37.625107	15.051082
	H	12.656804	41.081609	13.048634
	H	11.769411	39.732698	14.893497
	H	11.221817	38.91852	13.432641
	H	11.022398	37.689059	15.717828
	H	12.762109	37.568008	15.687469
	H	12.987417	39.00472	10.898897
	H	14.062763	39.434506	14.38919

	H	13.765713	38.265405	13.116523
	C	11.75357	36.362092	14.180327
	N	10.399182	36.130845	13.615741
	H	12.440914	36.414446	13.350451
	H	11.981502	35.48992	14.772976
	H	10.337523	35.214501	13.163105
	C	-0.570526	32.616672	10.481896
	C	-1.677281	31.599262	10.117566
	C	-3.069135	32.201215	10.098807
	C	-3.090784	33.264899	9.018764
	C	-1.949069	34.256404	9.134737
	C	-0.797647	33.990833	9.812878
	C	0.227038	35.058086	9.956395
	C	1.395134	35.050684	10.644256
	C	2.381582	36.141492	10.700439
	C	3.535848	35.905584	11.384553
	C	4.686475	36.784715	11.592398
	C	5.836888	36.29476	12.120501
	C	7.061232	37.038285	12.449803
	C	8.115216	36.32779	12.940523
	C	9.348567	36.864895	13.496754
	C	0.740278	31.95696	10.017124
RET	C	-0.576355	32.79861	12.010376
	C	-2.299925	35.566036	8.457608
	C	2.087465	37.422612	9.962167
	C	7.105404	38.518563	12.173817
	H	9.365236	37.861693	13.890488
	H	8.052803	35.257141	12.947428
	H	5.867746	35.245707	12.344206
	H	4.603212	37.823976	11.331823
	H	3.644807	34.928315	11.824305
	H	1.685662	34.191913	11.210284
	H	-0.010102	35.968643	9.446315
	H	2.945195	38.077214	9.959835
	H	1.834226	37.219614	8.927291
	H	1.249046	37.950498	10.411718
	H	8.013277	38.98688	12.530105
	H	7.060439	38.673356	11.101352
	H	6.258229	39.030614	12.607782
	H	-2.970933	36.135282	9.096236
	H	-1.459439	36.194552	8.204348
	H	-2.836583	35.363086	7.533572
	H	1.629467	32.494414	10.296841
	H	0.815162	30.964017	10.446547

	H	0.748919	31.842726	8.940758
	H	0.119732	33.547801	12.353735
	H	-1.553865	33.106462	12.348315
	H	-0.321176	31.860876	12.497401
	H	-4.023087	33.809755	9.0432
	H	-3.070356	32.78602	8.040675
	H	-3.819006	31.445724	9.890718
	H	-3.310974	32.639564	11.063218
	H	-1.478249	31.191511	9.129855
	H	-1.612564	30.758307	10.80278
	O	9.093849	31.860766	12.361789
WAT619	H	9.420837	32.781281	12.119944
	H	9.998057	31.479714	12.525309

Table S17: Coordinates of the ^1B_u-CASSCF optimised geometry

Resdiue Name	Atom Name	x	y	z
	N	12.699263	39.908138	11.279383
	C	13.282307	40.29548	12.582986
	C	14.603443	41.002965	12.405384
	O	14.764759	42.143053	12.796293
	C	13.344225	39.099929	13.56503
	C	11.952862	38.8701	14.195767
	C	11.813246	37.562826	14.996525
LYP	H	12.651584	41.044789	13.068448
	H	11.769064	39.681353	14.896111
	H	11.192163	38.926768	13.418483
	H	10.991875	37.660696	15.707749
	H	12.713833	37.438762	15.59091
	H	12.966587	39.006769	10.899405
	H	14.050369	39.325753	14.364778
	H	13.70192	38.200805	13.060777
	C	11.584336	36.330045	14.113384
	N	10.18552	35.937498	14.053585
	H	11.979312	36.512183	13.119946
	H	12.118091	35.49701	14.543517
	H	10.082768	34.942358	13.969365
RET	C	-0.590269	32.626758	10.48202
	C	-1.709471	31.597217	10.134055
	C	-3.093117	32.241964	10.110961
	C	-3.07624	33.285069	8.997811
	C	-1.958155	34.297205	9.146756
	C	-0.795266	33.999002	9.832199
	C	0.20568	35.049361	9.972815

	C	1.402757	35.060412	10.655224
	C	2.337048	36.140046	10.67336
	C	3.538622	35.904682	11.36204
	C	4.622368	36.766037	11.537511
	C	5.800947	36.280656	12.129919
	C	6.988494	36.992133	12.403862
	C	8.053303	36.241601	12.977844
	C	9.254371	36.71966	13.478818
	C	0.708801	31.92469	10.011799
	C	-0.581147	32.789048	12.020622
	C	-2.298333	35.617243	8.488909
	C	2.072958	37.416488	9.920527
	C	7.121324	38.448006	12.040364
	H	9.444308	37.7706	13.478351
	H	7.927001	35.179745	13.004415
	H	5.790069	35.243756	12.401736
	H	4.571048	37.788064	11.214033
	H	3.64954	34.922367	11.785911
	H	1.723864	34.226777	11.244239
	H	-0.027556	35.960504	9.46805
	H	2.964444	38.016289	9.841322
	H	1.73506	37.204469	8.914423
	H	1.305639	37.998804	10.423127
	H	8.150118	38.767816	12.091188
	H	6.780835	38.620861	11.025028
	H	6.536461	39.086001	12.694331
	H	-3.135109	36.073712	9.011655
	H	-1.50179	36.34135	8.453428
	H	-2.627468	35.451503	7.465076
	H	1.618418	32.469974	10.224602
	H	0.81105	30.953278	10.496464
	H	0.687095	31.756352	8.937041
	H	0.122034	33.53131	12.386917
	H	-1.55895	33.113336	12.360743
	H	-0.338519	31.847059	12.510718
	H	-4.036803	33.788926	9.00334
	H	-3.009662	32.795933	8.022564
	H	-3.860335	31.493332	9.906461
	H	-3.328363	32.705692	11.070838
	H	-1.530482	31.161369	9.147834
	H	-1.701728	30.761629	10.837433
	O	9.295719	32.050658	12.444386
WAT619	H	9.620581	32.981191	12.222325
	H	10.197998	31.681238	12.630337

Table S18: Coordinates of the S_0-CASSCF optimised geometry in alternative protonation

Residue Name	Atom Name	x	y	z
E162	N	7.454168	32.338145	19.894443
	H	7.594888	31.385416	19.576235
	C	8.372837	33.370888	19.378397
	H	8.895933	33.81765	20.227404
	C	9.423348	32.7361	18.429873
	H	10.056049	32.057481	19.006508
	H	8.898369	32.113268	17.713873
	C	10.330742	33.737398	17.660375
	H	9.862453	34.707891	17.514624
	H	11.236877	33.91737	18.243062
	C	10.695253	33.236953	16.276585
	O	10.063621	32.492956	15.55614
	O	11.895784	33.66456	15.844987
	H	11.998762	33.398403	14.893406
	C	7.61186	34.479975	18.673354
	O	7.942691	35.643367	18.800039
D292	N	12.077763	34.838838	9.053952
	H	12.200762	33.849263	8.87478
	C	12.527734	35.326959	10.380488
	H	11.717672	35.907626	10.822158
	C	12.933212	34.205847	11.393635
	H	13.419633	33.38825	10.865817
	H	13.687379	34.611665	12.073176
	C	11.80867	33.646209	12.284256
	O	12.092512	33.07285	13.365946
	O	10.611971	33.946964	12.071426
	C	13.707058	36.272349	10.205243
	O	13.783344	37.320359	10.816756
LYP	N	12.716996	39.891522	11.290442
	C	13.306607	40.334454	12.579475
	C	14.623892	41.024192	12.376881
	O	14.789398	42.170613	12.743492
	C	13.39578	39.206442	13.62444
	C	12.002092	38.961658	14.239907
	C	11.882973	37.614455	14.953654
	H	12.684822	41.10591	13.042271
	H	11.794494	39.735444	14.972956
	H	11.244323	39.0327	13.459561
	H	11.018133	37.609511	15.620342
	H	12.762193	37.477956	15.57688
	H	13.027982	39.008642	10.897604

	H	14.080206	39.499127	14.422635
	H	13.81446	38.308735	13.170124
RET	C	11.760094	36.481007	13.927851
	N	10.373782	36.18388	13.507806
	H	12.340191	36.70239	13.045638
	H	12.146995	35.578276	14.361164
	H	10.293085	35.250467	13.103633
	C	-0.589657	32.611923	10.476188
	C	-1.696573	31.597415	10.105664
	C	-3.086569	32.203901	10.079702
	C	-3.1034	33.267721	8.999767
	C	-1.959794	34.254829	9.11943
	C	-0.81379	33.984307	9.803844
	C	0.208477	35.049162	9.951137
	C	1.368411	35.039335	10.650085
	C	2.353923	36.126744	10.705666
	C	3.499529	35.890083	11.402001
	C	4.644424	36.770255	11.596972
	C	5.797957	36.291821	12.126318
	C	7.012452	37.052606	12.414271
	C	8.090515	36.361584	12.883136
	C	9.331483	36.927379	13.347701
	C	0.723866	31.949874	10.021939
	C	-0.601778	32.79502	12.004546
	C	-2.298571	35.566739	8.440578
	C	2.075263	37.403012	9.953983
	C	7.032679	38.528561	12.122882
	H	9.383396	37.957681	13.633762
	H	8.043069	35.289379	12.901671
	H	5.838703	35.24656	12.365361
	H	4.562063	37.804214	11.318656
	H	3.60476	34.916582	11.850484
	H	1.651847	34.182584	11.222033
	H	-0.019328	35.958228	9.434766
	H	2.933197	38.057359	9.957487
	H	1.837169	37.191496	8.917848
	H	1.231607	37.934722	10.387731
	H	7.928349	39.02106	12.47583
	H	6.988031	38.668736	11.049047
	H	6.17418	39.025109	12.550881
	H	-2.961805	36.143777	9.080068
	H	-1.452329	36.186262	8.183474
	H	-2.838313	35.367831	7.518106
	H	1.613645	32.482395	10.309953

	H	0.790944	30.957009	10.45258
	H	0.744278	31.835485	8.94625
	H	0.078017	33.558077	12.350219
	H	-1.585293	33.084154	12.34029
	H	-0.327894	31.862877	12.492149
	H	-4.033493	33.81557	9.024049
	H	-3.081853	32.790798	8.02103
	H	-3.83752	31.451193	9.868589
	H	-3.330803	32.643299	11.042866
	H	-1.492496	31.189735	9.119131
	H	-1.638721	30.756135	10.790895
	O	9.330669	31.866132	12.953708
WAT619	H	9.850373	32.551087	12.454745
	H	9.593001	32.106618	13.864621

Table S19: Coordinates of the ^1B_u-CASSCF optimised geometry at $P_{[-97]}$+

Residue Name	Atom Name	x	y	z
	N	12.697681	39.892355	11.268457
	C	13.277806	40.235143	12.584291
	C	14.603047	40.955093	12.443931
	O	14.76394	42.069567	12.898338
	C	13.313324	39.010698	13.538448
	C	11.922265	38.807145	14.184493
	C	11.793909	37.571018	15.09247
	H	12.643948	40.975293	13.076974
LYP	H	11.744166	39.66183	14.8305
	H	11.143997	38.795719	13.417254
	H	10.940773	37.697201	15.755262
	H	12.670106	37.519709	15.734574
	H	12.976601	39.009465	10.855149
	H	14.033068	39.200835	14.334338
	H	13.644223	38.110844	13.018182
	C	11.635023	36.269193	14.313418
	N	10.388247	36.192892	13.560394
	H	12.432405	36.177204	13.592908
	H	11.687396	35.428982	14.964063
	H	10.472368	35.577331	12.753421
	C	-0.642928	32.602616	10.501469
RET	C	-1.806515	31.615381	10.171025
	C	-3.166235	32.311885	10.131982
	C	-3.12445	33.305383	8.974414
	C	-1.9842	34.290769	9.099658
	C	-0.791652	33.96982	9.82992

	C	0.225601	34.987909	9.973427
	C	1.418287	34.976256	10.672838
	C	2.381072	36.058254	10.749327
	C	3.59388	35.795788	11.503767
	C	4.635695	36.670017	11.71445
	C	5.871732	36.301284	12.338505
	C	6.989535	37.164754	12.376272
	C	8.359803	36.717754	12.661629
	C	9.186865	36.675015	13.793315
	C	0.627705	31.845264	10.04229
	C	-0.623463	32.791345	12.037892
	C	-2.2674	35.611574	8.421951
	C	2.203944	37.310884	9.93236
	C	6.898148	38.575323	11.858549
	H	8.957824	37.112097	14.743589
	H	8.927526	36.446021	11.803908
	H	5.977347	35.29456	12.683184
	H	4.546704	37.67517	11.350221
	H	3.688957	34.800842	11.904636
	H	1.714764	34.127648	11.257567
	H	0.013854	35.908595	9.472844
	H	3.150094	37.800397	9.748309
	H	1.771026	37.088026	8.964328
	H	1.549795	38.025231	10.430717
	H	7.829419	39.107817	12.004838
	H	6.664958	38.593828	10.798562
	H	6.119465	39.114909	12.37956
	H	-3.050878	36.143693	8.958618
	H	-1.419517	36.272119	8.340628
	H	-2.643088	35.450125	7.412113
	H	1.550583	32.393652	10.181614
	H	0.728019	30.912367	10.596096
	H	0.567825	31.600237	8.983267
	H	0.059969	33.558881	12.388417
	H	-1.604804	33.100835	12.375412
	H	-0.355465	31.866282	12.545502
	H	-4.066735	33.837483	8.954889
	H	-3.06493	32.779078	8.018762
	H	-3.965621	31.587598	9.969911
	H	-3.367754	32.828292	11.071904
	H	-1.64733	31.153263	9.19421
	H	-1.831269	30.793448	10.888053
WAT619	O	9.315831	31.957441	12.448486
	H	9.622643	32.899203	12.30005

	H	10.217794	31.564522	12.551456

Table S20: Coordinates of the ^1B_u-CASSCF optimised geometry at $P_{[-247]}$-

Residue Name	Atom Name	x	y	z
LYP	N	12.700757	39.915145	11.280009
	C	13.280374	40.31623	12.579004
	C	14.598392	41.025491	12.38345
	O	14.756504	42.171745	12.756142
	C	13.405387	39.116882	13.537939
	C	12.035176	38.653536	14.087398
	C	12.163349	37.292462	14.807039
	H	12.63888	41.044661	13.083659
	H	11.67986	39.390566	14.809025
	H	11.294464	38.600541	13.285398
	H	11.752373	37.356885	15.818053
	H	13.21588	37.068747	14.902462
	H	12.995771	39.029763	10.886056
	H	14.03396	39.405102	14.382619
	H	13.910801	38.293145	13.030491
RET	C	11.51894	36.136858	14.043499
	N	10.07221	36.18836	14.217257
	H	11.747679	36.228031	12.9987
	H	11.88017	35.193424	14.422811
	H	9.72467	36.143718	15.156813
	C	-0.551165	32.605182	10.428974
	C	-1.635986	31.556864	10.037506
	C	-3.047042	32.144886	10.053907
	C	-3.104952	33.222791	8.97437
	C	-2.018913	34.265648	9.124667
	C	-0.796754	33.985741	9.813862
	C	0.165401	35.056818	9.963166
	C	1.369081	35.09012	10.632033
	C	2.311343	36.190767	10.65944
	C	3.566653	35.919689	11.317628
	C	4.648941	36.759407	11.474996
	C	5.810304	36.335675	12.182681
	C	6.903608	37.16198	12.519175
	C	7.892439	36.703557	13.51343
	C	9.234119	36.392793	13.240659
	C	0.773098	31.957246	9.949446
	C	-0.554365	32.720183	11.971447
	C	-2.384219	35.595214	8.504775
	C	2.047126	37.472537	9.919351

	C	6.924825	38.634629	12.196385
	H	9.629509	36.389359	12.246478
	H	7.625457	36.767514	14.557136
	H	5.834301	35.315659	12.512378
	H	4.610827	37.762459	11.094794
	H	3.663138	34.932504	11.737211
	H	1.707591	34.260184	11.21803
	H	-0.099462	35.973741	9.482232
	H	2.965452	38.008709	9.728003
	H	1.581422	37.28635	8.958754
	H	1.38658	38.126881	10.487535
	H	7.558797	39.180685	12.885104
	H	7.303781	38.806139	11.19441
	H	5.931845	39.054503	12.255001
	H	-3.178609	36.067804	9.078306
	H	-1.573532	36.301465	8.43217
	H	-2.771332	35.452948	7.496722
	H	1.666753	32.488541	10.246637
	H	0.874238	30.947843	10.347665
	H	0.791844	31.888679	8.86561
	H	0.159149	33.44297	12.357494
	H	-1.530308	33.045652	12.322035
	H	-0.320089	31.759133	12.428022
	H	-4.080665	33.692652	9.026983
	H	-3.048793	32.770192	7.981373
	H	-3.783657	31.369968	9.840029
	H	-3.287764	32.567405	11.031334
	H	-1.442141	31.178763	9.030661
	H	-1.592335	30.690782	10.702175
	O	9.324117	32.024062	12.433215
WAT619	H	9.619035	32.976631	12.282609
	H	10.242439	31.655257	12.51773

Table S21: Coordinates of the 13-*cis* S_0-CASSCF optimised geometry

Residue Name	Atom Name	x	y	z
	N	7.476169	32.353561	19.922919
	H	7.647083	31.413108	19.582817
	C	8.375742	33.424104	19.419453
	H	8.875477	33.885882	20.27363
	C	9.475116	32.911436	18.453296
E162	H	10.133789	32.222074	18.986466
	H	8.994917	32.34255	17.658467
	C	10.333035	34.053851	17.83038
	H	9.709864	34.841779	17.403657
	H	10.944933	34.517125	18.608265

	C	11.20061	33.562537	16.693723
	O	10.699379	32.747723	15.886572
	O	12.364419	34.005756	16.597631
	C	7.591936	34.511513	18.716547
	O	7.859022	35.684672	18.887027
D292	N	12.060627	34.844974	9.040786
	H	12.175477	33.851702	8.879329
	C	12.514936	35.352081	10.356524
	H	11.709889	35.945361	10.784809
	C	12.847322	34.222541	11.367216
	H	13.55264	33.529497	10.906037
	H	13.36272	34.648752	12.229107
	C	11.619986	33.447365	11.873598
	O	11.774205	32.303274	12.369999
	O	10.496299	34.01303	11.83427
	C	13.699281	36.28358	10.202187
	O	13.76908	37.352849	10.779872
LYP	N	12.698514	39.906623	11.287779
	C	13.293131	40.351013	12.572467
	C	14.60401	41.052854	12.352634
	O	14.761425	42.212013	12.682455
	C	13.406377	39.2074	13.603518
	C	12.043767	38.968133	14.286091
	C	11.946442	37.638598	15.065349
	H	12.669624	41.116476	13.044208
	H	11.861139	39.76691	14.996252
	H	11.245952	39.049848	13.547609
	H	11.068491	37.687738	15.710922
	H	12.808859	37.558199	15.717871
	H	13.030677	39.036596	10.883897
	H	14.131058	39.487143	14.370392
	H	13.780939	38.303156	13.124618
RET	C	11.804895	36.405234	14.147099
	N	10.701371	36.667098	13.220045
	H	12.709975	36.273272	13.577256
	H	11.62014	35.518674	14.731519
	H	10.894454	37.410703	12.570629
	C	-0.399278	32.630029	10.481953
	C	-1.559916	31.725422	10.014693
	C	-2.912891	32.412403	10.059444
	C	-2.877407	33.599909	9.111805
	C	-1.63905	34.460808	9.25572
	C	-0.51224	34.049302	9.897421
	C	0.583166	35.02825	10.095723

	C	1.729935	34.922216	10.809704
	C	2.751339	35.967624	10.934012
	C	3.903156	35.66289	11.598538
	C	5.000364	36.586037	11.806985
	C	6.240287	36.311892	12.28806
	C	7.245847	37.369998	12.332739
	C	8.553831	37.321538	12.6879
	C	9.450328	36.36452	13.301632
	C	0.88052	31.918908	10.010904
	C	-0.445183	32.724649	12.018198
	C	-1.823413	35.855942	8.683935
	C	2.47819	37.29833	10.272126
	C	6.812054	38.727483	11.849663
	H	9.167358	35.525407	13.906089
	H	9.072135	38.246666	12.531348
	H	6.521133	35.313667	12.550938
	H	4.794271	37.596371	11.533629
	H	4.02468	34.66218	11.968468
	H	1.968298	34.027203	11.340846
	H	0.417231	35.970599	9.616382
	H	3.296746	37.990919	10.378482
	H	2.308604	37.162822	9.208787
	H	1.589584	37.76342	10.691566
	H	5.941613	39.067446	12.390134
	H	7.590512	39.46385	11.989274
	H	6.561453	38.690256	10.796861
	H	-2.02325	36.569284	9.479283
	H	-0.967733	36.212157	8.123385
	H	-2.673954	35.871878	8.009854
	H	1.790445	32.409968	10.302556
	H	0.914225	30.914877	10.417269
	H	0.894476	31.828249	8.932909
	H	0.301018	33.39542	12.41792
	H	-1.40242	33.094921	12.355857
	H	-0.281247	31.742017	12.454463
	H	-3.739068	34.234111	9.271811
	H	-2.965998	33.246147	8.084951
	H	-3.704557	31.729426	9.767111
	H	-3.13376	32.749299	11.068381
	H	-1.373575	31.409778	8.990946
	H	-1.553913	30.817903	10.613601
	O	9.138441	31.897296	12.397368
WAT619	H	9.420287	32.814175	12.075477
	H	10.069598	31.592059	12.592993